

Review

Ice Microstructure and Fabric of Guliya Ice Cap in Tibetan Plateau, and Comparisons with Vostok3G-1, EPICA DML, and North GRIP

Yuan Li ^{1,3,*}, Sepp Kipfstuhl ^{2,†} and Maohuan Huang ^{1,†}

¹ State Key Laboratory of Cryospheric Sciences, Northwest Institute of Eco-Environment and Resources, Chinese Academy of Sciences, Lanzhou 730000, China; huangmaohuan@sina.com

² Alfred Wegener Institute for Polar and Marine Research, Columbusstrasse, D-27568 Bremerhaven, Germany; Sepp.Kipfstuhl@awi.de

³ University of Chinese Academy of Sciences, Beijing 100049, China

* Correspondence: liyuan0614@163.com; Tel.: +86-180-5214-1206

† These authors contributed equally to this work.

Academic Editors: Helmut Cölfen and Mei Pan

Received: 17 January 2017; Accepted: 22 March 2017; Published: 30 March 2017

Abstract: This work is the first in the general natural ice literature to compare microstructures and fabrics of continent-type mountain ice in mid-low latitudes with polar ice in order to find out how they evolved based on similar fabric patterns of their vertically girdles. Microstructures and fabrics along the Guliya ice core on the Tibetan Plateau, China, were measured at a depth interval of approximately 10 m. The grain sizes increase unevenly with depth. The fabric patterns vary from the isotropic fabric, to broad single maximum, to vertical girdle, to single-maximum, and finally to multiple-maximum fabric. The grain growth rate of the Guliya core is faster than that of the Vostok3G-1, the EPICA DML, and the North GRIP. The vertical girdle fabric of the Guliya core forms at a high temperature and low strain rate. The strong single maximum fabric of the Guliya core appears in the mid-low part of the core with vertical uniaxial compression or simple shear. The thermal kinematics caused by the temperature can play a vital role in different stress cases to cast the similar or same fabric patterns. Normal grain growth, polygonization/rotation recrystallization, and migration recrystallization play roles of different importance at different depths.

Keywords: microstructure; fabric; ice cap; tripartite paradigm

1. Introduction

The ensemble of *c*-axis orientations (the *c*-axis of each grain points in a direction given by a unit vector \vec{c} within a mass of polycrystalline ice) constitutes the *c*-axis fabric of the ice, sometimes referred to as orientation fabric, or simply ‘fabric’ [1]. The distribution of grain and sub-grain sizes and shapes, and the misorientation of neighboring grains in polycrystalline ice, comprise the microstructure [1–6]. Both grain-scale structural characteristics impact on the micro- and macro-stress and strain states during deformation and recrystallization of ice. In turn, the deformation and the recrystallization supply information on the operation of processes of the microstructure and fabric [5]. Ice microstructure and fabric can reveal, to some extent, the rheology of natural ice concerning the history of climate change. Some micro-processes, such as lattice dislocation, intra-grain sliding, and diffusion creep with respect to the temperature of ice since its formation can be used to deduce inversely the paleo-air-temperature, ice-flow control laws, *c*-axis fabrics, and grain sizes. For this reason, constructing the relationship between the evolution of microstructure and fabric and climate change [6–13] is meaningful work, even though it is challenging and complex. Ice microstructure

and fabrics have been measured and analyzed with fruitful results in polar areas in Antarctica and Greenland [5,14–21]. However, few reports on mountain ice, especially from west China, have been published. Given that the Guliya mountain glacier manifested a vertical girdle fabric phenomena [22] similar to sites at the Vostok3G-1 (Former Soviet Antarctic station [23]), the EPICA DML (European Project for Ice Coring in Antarctica, Dronning Maud Land, [5,20,24–26]), and the North GRIP (North Greenland Ice core Project, [17,27–29]), this study may be of broad interest. This article aims first to compare microstructures and fabrics in continent-type mountain ice in mid-low latitudes with polar ice to explore the general ice literature on natural ice [30,31].

The Guliya ice cap (35°21' N, 81°31' E, c.6200 m a.s.l.) which is located in the western part of the Western Kunlun Mountains, on the Tibetan Plateau, China (Figure 1a) is the highest (average elevation is 6700 m), largest (total area c.376.05 km², top-flatted area c.131.75 km²), thickest (average ice thickness c.200 m, the thickest c.350 m), and coldest (lowest air temperature −24.1 °C in May, mean monthly −17.8 °C, −15.6 °C 10 m below surface) continent-type ice cap in Central Asia [32]. There are c.4306 glacier tributaries covering c.8438 km² and occupying over 3/4 of the total area around the Kunlun Mountains. The 308.7 m-long ice core extracted by China (Lanzhou Institute of Glaciology and Geocryology, Chinese Academy of Sciences) in cooperation with the U.S.A (Byrd Polar Research Centre, Ohio State University) in 1992, extended to bedrock [32]. The borehole site was in the superimposed ice zone, in which the annual net accumulation rate was estimated to be 25.2 cm i.e., a⁻¹ (pers. commun. from Shi Weilin). The surface temperature was around −18.6 °C. The ice temperatures measured in the borehole were −15.6, −5.9, and −2.1 °C at depths of 10.0, 220.0, and 308.0 m, respectively. It was estimated by a laminar flow model that shear stress was 84 kPa at the bottom [22]. The age of this ice core determined by by ³⁶Cl [33] is estimated to more than 500 ka.

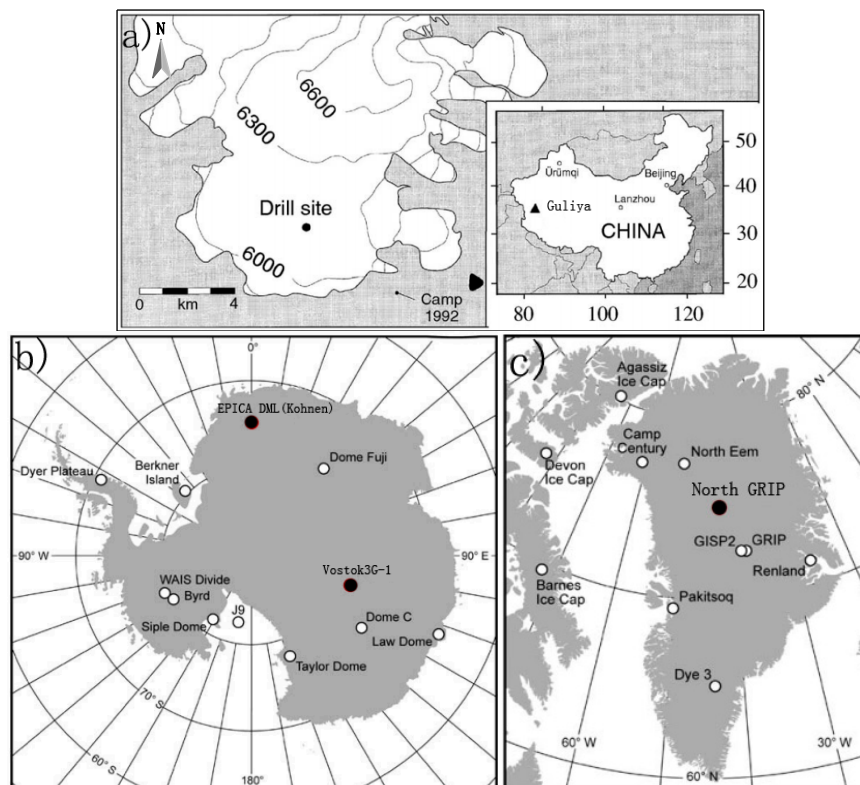


Figure 1. The sketches of the drilling sites of the ice cores for the Guliya, the Vostok3G-1, the EPICA DML, and the North GRIP. (a) The Guliya ice core (after [33]), (b) The Vostok3G-1 and the EPICA DML (adapted from Figure 15.1 of *The Physics of Glaciers* [1]) and (c) The North GRIP (adapted from Figure 15.1 of *The Physics of Glaciers* [1]).

The following three cores are compared with the Guliya ice core: the 2083 m long Vostok 3G-1 ice core (Figure 1b) and the 2774 m deep EPICA DML ice core from East Antarctica (Figure 1b), and the 3085 m long North GRIP on an ice ridge (Figure 1c) from Greenland (Table 1). They were drilled in the years 1980–1982, 2001–2006, and 1999–2001, respectively.

Table 1. Relevant information on ice cores presented in this text.

Ice Core Project	Geographical Site	Position	Elevation (m)	Topography	Ann. M S T(°C)/T 10 m B S or B (°C) †	Snow Accumulation Rate	Ice Core Length (m)/Ice Thickness (m)
Guliya	Western Kunlun Mountains, Tibetan Plateau, China	35°21' N, 81°31' E	6200	Ice cap top-flatted	−17.8/−15.6 (−10 m)	25.2 cm a ^{−1}	308.7/c.350
Vostok 3G-1	Former Soviet Antarctic station, Antarctica	78°28' S, 106°48' E	3488	Above an ice lake	−55.5/−3 (Bottom)	2.2–2.5 g cm ^{−2} a ^{−1}	2083/c.3700
EPICA DML	Interior of DML, Antarctica	75°00' S, 0°04' E	2892	Ridge/Divide	c.−45/c.−3 (Bottom)	6.4 g cm ^{−2} a ^{−1}	c.2774/2782
North GRIP	Ice ridge 325 km N-NW of Summit, Greenland	75°01' N, 42°03' W	2917	Ridge/Divide	−32/−2.4 (Bottom)	19.5 cm a ^{−1}	3085/3085

† Ann. M S T (°C)/T 10 m B S or B (°C) abbreviation indicates: Annual mean surface temperature (°C)/temperature 10 m below surface or bottom (°C).

2. Measurements

The ice of the Guliya core was placed in freezers at -18 °C during transportation from the Tibetan Plateau and stored in the cold laboratory at -18 °C until they were measured about six months after drilling (the properties of crystallography and mechanics were impacted indistinctively by this temperature because it was close to the average monthly temperature -17.8 °C [32]). Measurements of grain size and c-axis orientation were carried out in a cold room at -18 °C. Vertical thin sections were cut at a depth interval of ~ 10 m along the core axis, with a sampling rate of approximately 1%. Thin sections were typically 0.7 mm thick. The average grain diameters were calculated by linear intercept method [34] and a multiplication factor of 1.75 was adopted [22]. Ice crystallographic measurements were performed through thin sections produced using the standard microtoming technique [35]. If the grain number was not enough for statistics (100 grains), one or two thin sections were cut again in parallel. Despite following suggestions made at a workshop on the presentation of ice crystal data obtained with automatic fabric analyzers (University of Copenhagen, 2002), a fabric diagram size of 4×4 cm was used and 200 c-axis orientations were randomly selected from the measured ones and plotted in each fabric diagram [4], we suppose that the results of the Guliya and Vostok3G-1 core still clearly imply the general trend and make good statistical sense. The measurement of the c-axis, where the maximum error was 5° , was made on a Rigsby stage using the procedure outlined by Langway [35], and c-axis data were plotted on the lower hemisphere of the Schmidt net using the refraction corrections supplied by Kamb [36].

The Vostok3G-1 vertical thin sections [23] were determined by similar methods to that of the Guliya core.

The EPICA DML thin sections were prepared according to standard procedures using a microtome from horizontally ($0.5 \times 50 \times 50$ mm) and vertically cut samples ($0.5 \times 50 \times 100$ mm). The grain sizes and c-axis orientations were derived using an automatic fabric analyzer system [37] in a -20 °C ice laboratory [20].

The grain areas of the North GRIP core were obtained by counting the number of pixels within the individual grain boundaries from digital sample images of the fifteen 10×20 cm vertical thin sections, evenly distributed in the depth interval of 115–880 m [17]. C-axis orientations on vertical thin sections at 142 different depths between 100 m and 2930 m [27] were measured by an automatic ice-fabric analyzer [38].

3. Results

3.1. Microstructure and Fabric Variation with Depth

Both D_a (horizontal) and D_c (vertical) and the difference between them increase gradually in a general trend with depth in Figure 2. D_a is almost always larger than D_c at the same depth. The minimum mean grain diameter is ~ 5 mm at ~ 10 m depth and the maximum grain diameter exceeds 20 mm near the bottom. D_a is roughly close to D_c at several depths such as 63.0, 71.0, 101.0, and 121.0 m, which may indicate the existence of compression from the other two directions and also confirm the feasibility of calculating the grain size as a sphere shape. Results of c-axis statistics are plotted on the Schmidt diagrams and some typical results are shown in Figure 1 by Huang et al. [22]. The fabric patterns vary from isotropic fabrics in the upper 44 m to broad single maximum fabrics between 44 m and 63 m, to vertical girdles between 63 m and 167 m, and then to the sudden occurrence of strong single-maximum fabrics from 167 m to 203 m. Multiple-maximum fabrics occur in the remaining almost one-third of the core (Figure 3).

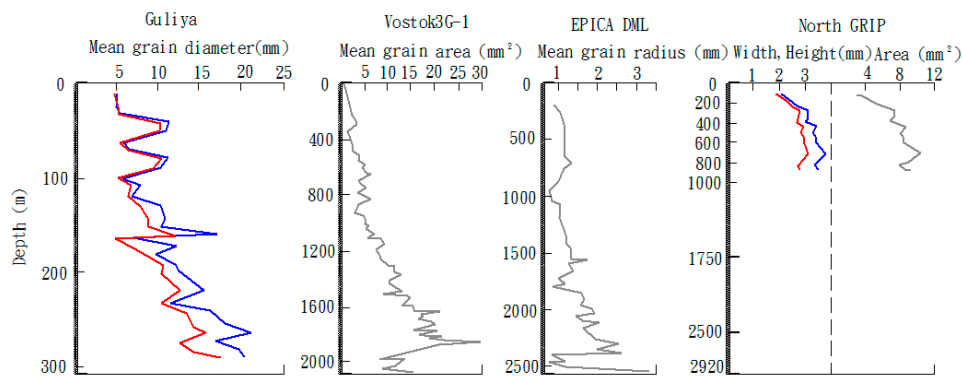


Figure 2. The profiles of the average grain size with depth for the Guliya, Vostok3G-1, EPICA DML, and North GRIP ice cores, respectively. D_a is the horizontal diameter (the red solid line), D_c the vertical diameter (the blue solid line) in the Guliya core. The red solid line is the width and the blue solid line is the height in the North GRIP core. Data are from [5,17,22,23], respectively.

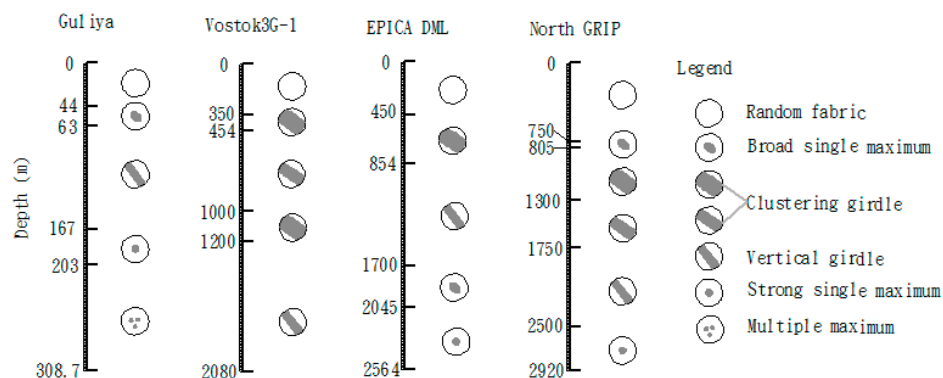


Figure 3. The sketches of evolution of fabric with depth for the Guliya, Vostok3G-13G-1, EPICA DML, and North GRIP ice cores, respectively. Data are from [20,22,23,27], respectively.

3.2. Comparison with the Vostok3G-1, EPICA DML, and North GRIP Ice Cores

Concerning the grain sizes: firstly, the grain area of the Vostok3G-1 core starts to grow by a significantly small ~ 0.5 mm² ($D \approx 0.8$ mm) on the surface, increases unevenly with depth, continuing to ~ 21 mm² ($D \approx 5.2$ mm) at ~ 1850 m, then enlarges abruptly to ~ 30 mm² ($D \approx 6.2$ mm) before decreasing steeply to ~ 6.5 mm² ($D \approx 2.8$ mm) at ~ 2000 m depth. Consequently, the average value in the

lowest tens of meters is $\sim 12 \text{ mm}^2$ ($D \approx 3.9 \text{ mm}$) (Figure 2). Below 100 m, grains appear to be elongated along a horizontal direction and a characteristic of the crystalline microstructure is the near absence of interpenetrating grains [23]. Secondly, the mean grain radius of the EPICA DML core has a general tendency to increase with depth (Figure 2). Faria et al. [30] state that, in the upper 700 m of the core, it increases with depth from $\sim 0.7 \text{ mm}$ at 100 m to $\sim 1.2 \text{ mm}$ at 700 m. Below that depth, it reduces markedly, reaching $\sim 0.5 \text{ mm}$ at 900 m depth and remaining small for a further 150 m. Grains become bigger again on average to more than 1.5 mm at $\sim 1700 \text{ m}$ depth. At depths of 1700–1850 m, grains get as small as 0.4 mm on average, and then resume growth reaching an average size of 2.5 mm at 2370 m depth. Below that point, the most extreme grain-size reduction takes place, with grains smaller than 0.3 mm on average within just around 30 m. Between the depths of 2400 m and 2500 m, the ice remains generally fine-grained, but the grain size varies more and the visual stratigraphy becomes severely disrupted. Below 2500 m, the ice temperature exceeds $-10 \text{ }^\circ\text{C}$ and grain sizes increase dramatically, reaching nearly 50 mm below 2600 m [5]. Thirdly, the mean grain area of the North GRIP core increases with depth towards a constant value (Figure 2), and the shape of the crystals becomes increasingly irregular [17]. The mean area displays a general but not very regular increase with depth, starting at $\sim 3.5 \text{ mm}^2$ ($D \approx 2.0 \text{ mm}$) at 100 m depth and leading to a limiting value for the older samples of $\sim 10 \text{ mm}^2$ ($D \approx 3.6 \text{ mm}$) at 700 m depth. The average grain width and height both follow the pattern of the mean grain area closely.

As to the fabric of the c-axes: firstly, in the upper 350 m of the Vistok3G-1 core, the c-axes appear to be quasi-uniformly distributed over the Schmidt equal-area net. A trend towards a clustering of c-axes around a vertical plane appears to start from a depth of 454 m and increases down to a depth of 1000 m [23]. However, at $\sim 1101 \text{ m}$ depth, this trend seems to expand slightly. Vertical girdles follow the fabric pattern above from $\sim 1200 \text{ m}$ to 2080 m near the bottom, and corresponding enhancements strengthen with depth (Figure 3). Secondly, the fabric of the EPICA DML core shows the depth evolution typical for an ice ridge [31]. The almost uniform distribution in the upper 450 m is followed by the continual development of a great circle girdle distribution down to 1700 m depth. Below that depth, a changeover region is formed towards an elongated vertical single maximum, which ends with a sudden collapse of the c-axes into a strong vertical single maximum at a depth of 2045 m [30] (Figure 3). Below 2564 m, grains become too large for the meaningful determination of c-axis distributions [39]. Thirdly, the fabric of the North GRIP core appears uniform in the uppermost 750 m (Figure 3). At a depth of 805 m, a broad single maximum has been formed, and at 1300–1750 m, a marked clustering of the c-axes towards the vertical plane is observed. This vertical girdle pattern strengthens further with depth, and persists down to 2500 m. Below 2500 m, the fabric transforms to a strong single maximum that displays variable strength down to 2920 m [27].

4. Discussion

4.1. Grain Growth

That the average grain size always increases with depth [22], is usually called grain growth. The grain growth is driven primarily by two factors: the curvature of energetic grain boundaries and the differences in stored strain energy among grains. The average grain size decreases or stops increasing by two processes: polygonization, where the existing grains are subdivided [8,15], and recrystallization, in which new grains are created [8]. The mean grain size of polycrystalline ice increases over time by grain growth in the absence of mechanisms to form new grains [1], i.e., the Normal Grain Growth (NGG) depends upon the migration which is driven by curvature of the boundaries in slowly deforming ice. In fact, processes of grain growth associated with rotation, polygonization, and recrystallization are active along the whole Guliya ice core, but different process contributes differently at different depth [2,5,40,41]. A general grain growth trend of the Guliya core (Figure 2)—the parabolic law [1]—indicates that the process of the NGG is active from top to bottom and overpowers the effects of polygonization and recrystallization as a whole [22]. We expect that the

NGG can take place along the whole Guliya core as the recrystallization is the same at all depths of the EPICA DML core [5]. This is different from the classical tripartite paradigm of the polar ice [8,15,42–46] which includes the NGG, the polygonization/rotation recrystallization (RRX), and the migration recrystallization (SIBM) from the top to the bottom down each core.

The average grain growth rate of the Guliya core is $0.72 \text{ mm}^2 \cdot \text{m}^{-1}$, two orders of magnitude larger than that of the Vostok3G-1 core ($0.006 \text{ mm}^2 \cdot \text{m}^{-1}$) [23]. The minimum grain diameter (around 5 mm) for the Guliya core is comparable to the largest grains for both Vostok3G-1 and EPICA DML cores (without taking into account the diameter of the lowest part (around 50 mm)), and larger than of the largest grains (around 3.6 mm) for the North GRIP core (without taking into account the core unmeasured, Figure 2). This suggests that the driving force for the grain growth of the Guliya mountain ice is far greater than that in the interior of polar regions. Within 10–101 m depth of the Guliya core, which possibly reflects periods of climatic warming and cooling (the grain diameter are evidently large at 44.0–51.0 m and 81.0–91.0 m, and distinctly small at 101.0 m in Figure 2) is consistent with the analysis of Lipenkov et al. [23] for the Vostok3G-1 core and Faria et al. [41] for the EPICA DML core, respectively. However, that the grain size of the Ice Age is significantly smaller than that of Holocene ice [8,27,30] has not been identified by the measurement of the Guliya ice core [22]. This can be explained by grains growing with age reaching a limited size where polygonization counteracts grain growth for the Holocene part of the EPICA DML core [20] and, by that, the grain growth of the North GRIP core for the last ~2 ka is seen to be linear with time, while the grains older than 2 ka merely approach a constant area (Figure 2), which is probably a result of polygonization [17]. Therefore, we consider that the polygonization might control the grain growth during the Holocene age of the Guliya core.

The grain growth of the Vostok3G-1 down to 2080 m is driven by the free energy of grain boundaries and in accordance with the low temperature and strain-rates [23]. The driving force for the migration of grain boundaries, and thus for grain growth of the EPICA DML core, cannot be the surface energy only, but is rather compounded from the grain-boundary surface energy and the stored strain energy [5]. Furthermore, the duration of the transformation of snow to ice in the Guliya core was generally less than one year, and was of warm type with the presence of melt water and thus coarse grains appeared in the surface layer [22]. Thus, we expect that the grain growth of the Guliya core is different from that of the Vostok3G-1, activated by the combination of static recrystallization and dynamic recrystallization which can occur in the uppermost part of the Guliya ice core.

4.2. Vertical Girdle

Firstly, the c-axis orientation of grains tends to orient perpendicular to the direction of the elongation of grains [47], forming a vertical girdle pattern. This type of fabric found on thin sections of the 63–167 m depth from the Guliya ice core (Figure 3; Figure 1 in [22]) have not been observed in other mountain ice in China. However, it has been reported in Antarctica, at the Vostok3G-1, where vertical girdles appear through to the bottom of the borehole from the depth of 454 m [23], at EPICA DML at 450–1700 m [5,20], and in Greenland, at the North GRIP, at 805–2500 m [17,27] (Figure 3). Furthermore, Fujita et al. [47], Lipenkov et al. [23], and Alley [7,8] perform computer simulation and explanation of vertical girdle formation. It is regarded as resulting from gradual rotation of grain by basal glide under uniaxial longitudinal tension, without recrystallization, at low temperature and strain rates. This is quite consistent with the formation mechanism of the vertical girdle for the Vostok3G-1 core [23,48]. On the one hand, along the section of the Guliya core with vertical girdle, the ice temperature is near $-10 \text{ }^\circ\text{C}$, where migration recrystallization can occur when the temperature is higher than $-10 \text{ }^\circ\text{C}$ [43]. The vertical girdles in the Guliya core are discontinuous, with other fabrics in between, showing that other processes of grain growth may overwhelm the action of the grain rotation [22]. Here, the RRX can be active due to the decrease of the grain diameter and the SIBM can also take place in the upper part of the 100-m depth with temperatures lower than $-10 \text{ }^\circ\text{C}$ [40], because boundaries of some grains appear interlocking and interfingering. Or the dynamic recrystallization by the non-basal sliding may

overtake the effect of the basal action [49] at high temperature—relative to the polar temperature. On the other hand, the vertical strain rate ($\dot{\epsilon}_{zz} = 0.52 \times 10^{-10} \text{ s}^{-1}$) is assumed to be a constant from top to bottom in a steady state of the Guliya core [22]. If the longitudinal strain rate $\dot{\epsilon}_{xx} = 2\dot{\epsilon}_{zz}$, then 610a is required to reach 100% of accumulated strain. Although the strain rate of the Guliya core is large as two orders of magnitude as that of the Vostok3G-1 core ($<10^{-12} \text{ s}^{-1}$) which is necessary for a vertical girdle to be well developed—an accumulated strain higher than 100%, which is in accordance with an age greater than 100 ka [23], it is compatible with low strain rates of the polar cores. So, we argue that the vertical girdle of the Guliya core may also be casted with dynamic recrystallization at high temperature and low strain rates.

Seddik et al. [20] demonstrated clearly that the girdle fabrics of the EPICA DML core produced a significantly different mechanical response depending on orientation relative to the ice flow. After deformation under uniaxial tension, the resulting fabric is a great circle perpendicular to the tensile axis—that is, similar to that exhibited by the Vostok3G-1 core—where converging flow is believed to occur [23]. Then, vertical girdles strengthened with depth for the North GRIP core tend to cluster around a vertical plane, indicating combined effects of vertical compression and horizontal tension from confined compression [17,27]. The most likely interpretation is that the c-axes rotate away from a horizontal-tension axis across the main ice divide, which runs N-NW-S-SE through the drilling site [27]. However, the ice flows hardly through horizontal directions on the top-flatted surface of the Guliya ice cap. This can be confirmed by the D_a close to D_c in the upper of the Guliya core (Figure 2). The hydrostatic pressure normal to the surface of the Guliya ice cap is less an order of magnitude than that of the North GRIP. Thus, we propose that the vertical girdle of the Guliya core may be related closely to the complex topography of the subglacier to make c-axes rotate away from an axis of horizontal tension. In other words, the vertical girdle can be created by two different orders of magnitude of deviatoric stresses. Or the thermal kinetics controlled by the temperature may also be an important factor to form the vertical girdle fabric of the Guliya core with different stress conditions of the polar ice.

The Vostok3G-1 ice hardens gradually with depth when considering the transverse convergent flow [23]. Some grains of the North GRIP core locate in a ‘hard’ position against vertical compression, but some are in a ‘soft’ one with their c-axes at or near 45° from the vertical compression axis [27]. We find that the ratio of tension strain against compression strain of the Guliya core intensifies with depth and it can be confirmed by the steadily increasing differences between D_a and D_c with depth (Figure 2). The ice softness implied by this ratio can contribute to the formation of the vertical girdle of the Guliya core. Thus, the static and dynamic grain growths co-operate to form the vertical girdle of the Guliya core through the degree of hardening and softening controlled by the delicate interplay of dislocation production, recovery, and dynamic recrystallization.

4.3. Simple Shear and Single-Maximum

Towards the base, the shear stress gradually increases due to the drag of the ice bed, finally exceeding the normal stress near the bed, and then the simple shear increases. The simple shear without recrystallization causes c-axis rotation from the normal toward the shear plane, forming a single maximum, while shear stress with recrystallization not only makes c-axes normal to the shear plane but forms sub-single-maximum in the shear direction. Azuma et al. [50] and Alley [7] show that the random fabric of polycrystalline ice is transformed into a broad single-maximum one when ice is deformed under uniaxial compression and the c-axis rotates away from the tensile axis. Firstly, based on thin sections from depths of 44.0 m to 63.0 m of the Guliya core, a broad single-maximum fabric initiates just from the random fabric (Figure 3). Gliding layers originate from the easiest deformation process, namely, the motion of dislocations on the basal plane. On the one hand, Lipenkov et al. [23] hold that, at very low strain rates ($<10^{-12} \text{ s}^{-1}$), the dislocation glide is the dominant deformation mode of the Vostok3G-1 ice for a broad single maximum fabric observed in the same core at 494 m by Barkov [51]. On the other hand, Weikusat et al. [5] argue that dislocation density decreasing processes

of the North GRIP core (recovery and dynamic recrystallization) play a far more important role under low stress conditions. Furthermore, by thin sections from depths of 167.0 m to 203.0 m of the Guliya core, a strong single-maximum fabric can be observed, *c*-axes are centered around the core axis—that is, normal to the shear plane—while sub-single-maximum are not significant. When the dislocation density decreases to be small enough with the formation of the single maximum fabric at the low strain rate, the NGG with diffusion creep may make the grain of the Guliya core enlarge meanly. Thus, the NGG and the dynamic recrystallization may contribute to the grain growth at the single maximum of the Guliya core.

A stable single-maximum fabric cannot form by grain rotation only [20]. Evidence of enhanced horizontal shear deformation rates of ice displaying a single-maximum fabric has been found by inclination measurements in the boreholes, and laboratory studies indicate that such ice is significantly more resilient to vertical compression than ice with a random fabric [52–56]. So, the single maximum seems to suggest that bed-parallel simple shear exerts a strong influence on the fabric in the 2500 m depth down to 2920 m of the North GRIP [27]. Significant changes in stress conditions near the bed can also lead to variations in fabric strength [57], but this is not likely to be important in the North GRIP region, where the ice-sheet bed is relatively flat [56,57]. Interestingly enough, a strong single maximum appearing in the lowest part of the North GRIP and the EPICA DML cores (Figure 3) suggests that simple shear deformation occurs near the ice bed [27,58]. However, a strong single maximum fabric exists in the mid-low part of the Guliya core. If the simple shear stress controls the single maximum, a complex topography of the ice bed can produce the difference of the shear stress between the ice layers. Otherwise, the single maximum can be formed by the vertical uniaxial compression instead of the simple shear.

4.4. Polygonization and Migration Recrystallization

Polygonization is the formation of new grains by subdividing the old grains. If different parts of a grain are subjected to different stress states, then the grain can become bent or twisted. Dislocations tend to organize between relative undeformed regions called sub-grains to form sub-grain boundaries that relieve this bending or twisting and lower the energy of the system. If a sub-grain boundary becomes sufficiently strong (or a sub-grain becomes sufficiently rotated), then the boundary becomes a full grain boundary. The polygonization can often be identified by the occurrence of more nearest-neighbor grains with small misorientation than random grains in a sample. Besides this, according to definition, in polygonization new grains form within a few degrees of old grains, so that the fabric is not affected greatly [8]. However, at the depth of 167 m of the Guliya core there are two fabric patterns: one exhibiting a vertical girdle, the other a strong single maximum. At the upper, non-polygonized part, 167a (Figure 1 in [22]), the average grain diameter is 14.7 mm, while the size at the lower, polygonized part, 167b (Figure 1 in [22]), is 5.8 mm. In 167a, the maximum concentration of *c*-axes is 17%, and in 167b it is 44%, accompanied by a steep reduction in mean grain diameter (Figure 2). This can be seen as the direct evidence of polygonization of the Guliya core.

As long as recrystallization processes do not occur intensively, it is possible that migration recrystallization causes multiple-maxima fabrics observed in high temperature ice [7]. However, the intensive recrystallization or convergent flow can lead the multiple-maximum to disappear at the Vostok3G-1 core, although the bottom temperature reaches $-3\text{ }^{\circ}\text{C}$ [23]. In addition, from the depth of 203 m until the base of the Guliya core, *c*-axis orientations center on the core axis, forming a multiple-maximum fabric of several clusters. This demonstrates the dominance of migration recrystallization because the temperature of over $-6\text{ }^{\circ}\text{C}$ at this depth exceeds $-10\text{ }^{\circ}\text{C}$ [43]. This can be confirmed by tendencies of second or multiple maxima with $-3\text{ }^{\circ}\text{C}$ observed at several depths at the EPICA DML [20] and by variations in the fabric strength below 2633 m due to various impurity contents, or to the onset of migration recrystallization at temperature higher than $-2.4\text{ }^{\circ}\text{C}$ near the bed, producing more open fabrics in the North GRIP core [44].

5. Conclusions

The grain growth rate of the Guliya core is faster than that of the Vostok3G-1, the EPICA DML and the North GRIP. The vertical girdle fabric of the Guliya core forms at high temperature and low strain rate rather than low temperature and strain rate as with Vostok3G-1. The strong single maximum fabric of the Guliya core appears in the mid-low part of the core with the vertical uniaxial compression or simple shear, rather than the bottom as the EPICA DML and the North GRIP with simple shear.

Similar or same fabrics with different geographic and climatic conditions between the Guliya and other three cores cannot be explained by the stress system alone. The thermal kinematics caused by the temperature can play a vital role in casting the fabric patterns in different stress cases.

The evolutions of ice microstructure and fabric with increasing depth to the Guliya core are not suitable to be addressed preferably by the classical tripartite paradigm of the polar ice—the NGG, RRX, and SIBM—from the surface to the bed. Each of the three roles can occur in all levels of the Guliya core, but they have a different importance at different depths.

Acknowledgments: We thank the Academic Editors: Helmut Cölfen and Mei Pan and two anonymous reviewers for their comments that improved the manuscript. We also thank all participants in the Guliya 1992 field project. The work presented here was supported by the National Basic Research Program of China (Grant No. 2013 CBA01804). We received funds for covering the costs to publish in open access. All sources of funding of the study should be disclosed. Please clearly indicate grants that you have received in support of your research work. Clearly state if you received funds for covering the costs to publish in open access.

Author Contributions: Yuan Li conceived and designed the structure of this paper; Yuan Li, Sepp Kipfstuhl and Maohuan Huang analyzed the data; Yuan Li wrote the paper.

Conflicts of Interest: The authors declare no conflict of interest.

References

1. Cuffey, K.M.; Paterson, W.S.B. *The Physics of Glaciers*, 4th ed.; Butter Worth Heinemann: Oxford, UK, 2010.
2. Kipfstuhl, S.; Hamann, I.; Lambrecht, A.; Freitag, J.; Faria, S.H.; Grigoriev, D.; Azuma, N. Microstructure mapping: A new method for imaging deformation-induced microstructural features of ice on the grain scale. *J. Glaciol.* **2006**, *52*, 398–406. [[CrossRef](#)]
3. Thorsteinsson, T. Fabric development with nearest-neighbour interaction and dynamic recrystallization. *J. Geophys. Res.* **2002**, *107*. [[CrossRef](#)]
4. Wang, Y.; Kipfstuhl, S.; Azuma, N.; Thorsteinsson, T.; Miller, H. Ice-fabrics study in the upper 1500 m of the Dome C (East Antarctica) deep ice core. *Ann. Glaciol.* **2003**, *37*, 97–104. [[CrossRef](#)]
5. Weikusat, I.; Kipfstuhl, S.; Faria, S.H.; Azuma, N.; Miyamoto, A. Subgrain boundaries and related microstructural features in EDML (Antarctica) deep ice core. *J. Glaciol.* **2009**, *55*, 461–472. [[CrossRef](#)]
6. Kennedy, J.H.; Pettit, E.C. The response of fabric variations to simple shear and migration recrystallization. *J. Glaciol.* **2015**, *61*, 537–550. [[CrossRef](#)]
7. Alley, R.B. Fabrics in polar ice sheets—Development and prediction. *Science* **1988**, *240*, 493–495. [[CrossRef](#)] [[PubMed](#)]
8. Alley, R.B. Flow-law hypotheses for ice-sheet modeling. *J. Glaciol.* **1992**, *38*, 245–256. [[CrossRef](#)]
9. Castelnau, O.; Canova, G.R.; Lebensohn, R.A.; Duval, P. Modeling viscoplastic behavior of anisotropic polycrystalline ice with a self-consistent approach. *Acta Mater.* **1997**, *45*, 4823–4834.
10. Faria, S.H.; Ktitarev, D.; Hutter, K. Modeling evolution of anisotropy in fabric and microstructure of polar ice. *Ann. Glaciol.* **2002**, *35*, 545–555. [[CrossRef](#)]
11. Gagliardini, O.; Meyssonier, J. Lateral boundary conditions for a local anisotropic ice flow model. *Ann. Glaciol.* **2002**, *35*, 503–509. [[CrossRef](#)]
12. Gillet-Chaulet, F.; Gagliardini, O.; Meyssonier, J.; Montagnat, M.; Castelnau, O. A user-friendly anisotropic flow law for ice-sheet modeling. *J. Glaciol.* **2005**, *41*, 3–14. [[CrossRef](#)]
13. Durand, G.; Gillet-Chaulet, F.; Svensson, A.; Gagliardini, O.; Kipfstuhl, S.; Meyssonier, J.; Parrenin, F.; Duval, P.; Dahl-Jensen, D. Change in ice rheology during climate variations—implications for ice flow modeling and dating of the EPICA Dome C core. *Clim. Past* **2007**, *3*, 155–167. [[CrossRef](#)]

14. Langway, C.C., Jr.; Shoji, H.; Azuma, N. Crystal size and orientation patterns in the Wisconsin-age ice from Dye 3, Greenland. *Ann. Glaciol.* **1988**, *10*, 109–115. [[CrossRef](#)]
15. Thorsteinsson, T.; Kipfstuhl, J.; Miller, H. Microstructures and fabrics in the GRIP ice core. *J. Geophys. Res.* **1997**, *102*, 26583–26599. [[CrossRef](#)]
16. Gow, A.J.; Meese, D.A.; Alley, R.B.; Fitzpatrick, J.J.; Anandakrishnan, S.; Woods, G.A.; Elder, B.C. Physical and structural properties of the Greenland ice sheet project 2 ice core: A review. *J. Geophys. Res.* **1997**, *102*, 26559–26575. [[CrossRef](#)]
17. Svensson, A.; Schmidt, K.G.; Dahl-Jensen, D.; Johnsen, S.J.; Wang, Y.; Kipfstuhl, J.; Thorsteinsson, T. Properties of ice crystals in North GRIP late-mid Holocene ice. *Ann. Glaciol.* **2003**, *37*, 113–118. [[CrossRef](#)]
18. EPICA Community Members. Eight glacial cycles from an Antarctic ice core. *Nature* **2004**, *429*, 623–628.
19. Durand, G.; Svensson, A.; Persson, A.; Gagliardini, O.; Gillet-Chaulet, F.; Sjolte, J.; Montagnat, M.; Dahl-Jensen, D. Evolution of the microstructure along the EPICA Dome C Ice Core. *Low Temp. Sci.* **2009**, *68*, 91–105.
20. Seddik, H.; Greve, R.; Placidi, L.; Hamann, I.; Gagliardini, O. Application of a continuum-mechanical model for the flow of anisotropic polar ice to the EDML core, Antarctica. *J. Glaciol.* **2008**, *54*, 631–642. [[CrossRef](#)]
21. Azuma, N.; Wang, Y.; Yoshida, Y.; Narita, H.; Hondoh, T.; Shoji, H.; Watanabe, O. Crystallographic analysis of the Dome Fuji ice core. In *Physics of Ice Core Records*; Hondoh, T., Ed.; Hokkaido University Press: Sapporo, Japan, 2000.
22. Huang, M.H.; Gao, X.; Jin, Z.M. Ice microstructures and their development of an ice core extracted from the Guliya ice cap, Kunlun Mountains. *J. Glaciol. Geocryol.* **1995**, *17*, 39–44.
23. Lipenkov, V.Y.; Barkov, N.I.; Duval, P.; Pimienta, P. Crystalline texture of the 2083 m ice core at Vostok Station, Antarctica. *J. Glaciol.* **1989**, *35*, 392–398. [[CrossRef](#)]
24. EPICA Community Members. One-to-one coupling of glacial climate variability in Greenland and Antarctica. *Nature* **2006**, *444*, 195–197.
25. Huybrechts, P.; Rybak, O.; Pattyn, F.; Ruth, U.; Steinhage, D. Ice thinning, upstream advection, and non-climatic biases for the upper 89% of the EDML ice core from a nested model of the Antarctic ice sheet. *Clim. Past* **2007**, *3*, 577–589. [[CrossRef](#)]
26. Weikusat, I.; Kipfstuhl, S.; Azuma, N.; Faria, S.H.; Miyamoto, A. Deformation microstructures in an Antarctic ice core (EDML) and in experimentally deformed artificial ice. *Low Temp. Sci.* **2009**, *68*, 115–123.
27. Wang, Y.; Thorsteinsson, T.; Kipfstuhl, J.; Miller, H.; Dahl-Jensen, D.; Shoji, H. A vertical girdle fabric in the North GRIP deep ice core, North Greenland. *Ann. Glaciol.* **2002**, *35*, 515–520. [[CrossRef](#)]
28. Dahl-Jensen, D.; Gundestrup, N.S.; Miller, H.; Watanabe, O.; Johnsen, S.J.; Steffensen, J.P.; Clausen, H.B.; Svensson, A.; Larsen, L.B. The North GRIP deep drilling programme. *Ann. Glaciol.* **2002**, *35*, 1–4. [[CrossRef](#)]
29. Durand, G.; Persson, A.; Samyn, D.; Svensson, A. Relation between neighbouring grains in the upper part of the North GRIP ice core: Implications for rotation recrystallization. *Earth Planet. Sci. Lett.* **2008**, *265*, 666–671. [[CrossRef](#)]
30. Faria, S.H.; Weikusat, I.; Azuma, N. The microstructure of polar ice. Part I: Highlights from ice core research. *J. Struct. Geol.* **2014**, *61*, 2–20. [[CrossRef](#)]
31. Faria, S.H.; Weikusat, I.; Azuma, N. The microstructure of polar ice. Part II: State of the art. *J. Struct. Geol.* **2014**, *61*, 21–49. [[CrossRef](#)]
32. Yao, T.; Jiao, K.; Zhang, X.; Yang, Z. Study on the glaciology of Guliya ice cap. *J. Glaciol. Geocryol.* **1992**, *14*, 233–241.
33. Thompson, L.G.; Yao, T.; Davis, M.E.; Henderson, K.A.; Thompson, E.; Lin, P.N.; Beer, J.; Synal, H.A.; Cole-Dai, J.; Bolzan, J.F. Tropical climate instability: The Last Glacial Cycle from a Qinghai–Tibetan ice core. *Science* **1997**, *276*, 1821–1825. [[CrossRef](#)]
34. Pickering, F.B. *The Basis of Quantitative Metallography*; Metals and Metallurgy Trust for the Institute of Metallurgical Technicians: Whetsone, UK, 1976.
35. Langway, C.C., Jr. *Ice Fabrics and the Universal Stage*; SIPRE Technical Report 62; SIPRE: Vicksburg, MS, USA, 1958.
36. Kamb, B. Refraction corrections for universal stage measurements. I. Uniaxial crystals. *Am. Mineral.* **1962**, *47*, 227–245.
37. Wilson, C.J.L.; Russell-Head, D.S.; Sim, H.M. The application of an automated fabric analyzer system to the textural evolution of folded ice layers in shear zones. *Ann. Glaciol.* **2003**, *37*, 7–17. [[CrossRef](#)]

38. Wang, Y.; Azuma, N. A new automatic ice-fabric analyzer which uses imageanalysis techniques. *Ann. Glaciol.* **1999**, *29*, 155–162.
39. Faria, S.H.; Freitag, J.; Kipfstuhl, S. Polar ice structure and the integrity of ice core paleoclimate records. *Quat. Sci. Rev.* **2010**, *29*, 338–351. [[CrossRef](#)]
40. Kipfstuhl, S.; Faria, S.H.; Azuma, N.; Freitag, J.; Hamann, I.; Kaufmann, P.; Miller, H.; Weiler, K.; Wilhelms, F. Evidence of dynamic recrystallization in polar firn. *J. Geophys. Res.* **2009**, *114*, B05204. [[CrossRef](#)]
41. Faria, S.H.; Kipfstuhl, S.; Lambrecht, A. *The EPICA-DML Deep Ice Core*; Springer: Berlin/Heidelberg, Germany, 2014.
42. Alley, R.B.; Gow, A.J.; Meese, D.A. Mapping c-axis fabrics to study physical processes in ice. *J. Glaciol.* **1995**, *41*, 197–203. [[CrossRef](#)]
43. Duval, P.; Castelnau, O. Dynamic recrystallization of ice in polar ice sheets. *J. Phys. IV (Paris)* **1995**. [[CrossRef](#)]
44. De la Chapelle, S.; Castelnau, O.; Lipenkov, V.; Duval, P. Dynamic recrystallization and microstructure development in ice as revealed by the study of deep ice cores in Antarctica and Greenland. *J. Geophys. Res.* **1998**, *103*, 5091–5105. [[CrossRef](#)]
45. Duval, P.; Arnaud, L.; Brissaud, O.; Montagnat, M.; de la Chapelle, S. Deformation and recrystallization processes of ice from polar ice sheets. *Ann. Glaciol.* **2000**, *30*, 83–87. [[CrossRef](#)]
46. Montagnat, M.; Duval, P. Rate controlling processes in the creep of polar ice, influence of grain boundary migration associated with recrystallization. *Earth Planet. Sci. Lett.* **2000**, *183*, 179–186. [[CrossRef](#)]
47. Fujita, S.; Nakawo, M.; Mae, S. Orientation of the 700-m Mizuho core and its strain history. In Proceedings of the Ninth Symposium on Polar Meteorology and Glaciology, Tokyo, Japan, 1 December 1986; Matsuda, T., Ed.; National Institute of Polar Research: Tokyo, Japan, 1987; pp. 122–131.
48. Pimienta, P.; Duval, P. Rate controlling processes in the creep of polar glacier ice. *J. Phys. (Paris)* **1987**. [[CrossRef](#)]
49. Weikusat, I.; Miyamoto, A.; Faria, S.H.; Kipfstuhl, S.; Azuma, N.; Hondoh, T. Subgrain boundaries in Antarctic ice quantified by X-ray Laue diffraction. *J. Glaciol.* **2011**, *57*, 85–94. [[CrossRef](#)]
50. Azuma, N.; Higashi, A. Formation processes of ice fabric pattern in ice sheets. *Ann. Glaciol.* **1985**, *6*, 130–134. [[CrossRef](#)]
51. Barkov, N.I. Rezul'taty issledovaniya skvazhiny i ledyanogo kerna na Stantsii Vostok v 1970–1972 [Results of the study of the borehole and ice core at Vostok Station, 1970–1972]. *Materialy Glyatsiologicheskikh Issledovaniy Khronika Ohsuzhdeniya* **1973**, *22*, 77–81.
52. Dahl-Jensen, D.; Gundestrup, N.S. Constitutive properties of ice at Dye 3, Greenland. In *The Physical Basis of Ice Sheet Modelling—Symposium, Vancouver*; International Association of Hydrological Sciences Publication: Wallingford, UK, 1987; Volume 17, pp. 31–43.
53. Shoji, H.; Langway, C.C., Jr. Flow-law parameters of Dye 3, Greenland, deep ice core. *Ann. Glaciol.* **1988**, *10*, 146–150. [[CrossRef](#)]
54. Paterson, W.S.B. Why ice-age ice is sometimes “soft”. *Cold Reg. Sci. Technol.* **1991**, *20*, 75–98. [[CrossRef](#)]
55. Dahl-Jensen, D.; Thorsteinsson, T.; Alley, R.B.; Shoji, H. Flow properties of the ice from the Greenland Ice Core Project ice core: The reason for folds? *J. Geophys. Res. Atmos.* **1997**, *1022*, 26831–26840. [[CrossRef](#)]
56. Dahl-Jensen, D.; Gundestrup, N.; Keller, K.R.; Johnsen, S.J.; Gogineni, S.P.; Allen, C.T.; Chuah, T.S.; Miller, H.; Kipstuhl, S.; Waddington, E.D. A search in north Greenland for a new ice-core drill site. *J. Glaciol.* **1997**, *43*, 300–306. [[CrossRef](#)]
57. Budd, W.F.; Jacka, T.H. A review of ice rheology for ice sheet modelling. *Cold Reg. Sci. Technol.* **1989**, *16*, 107–144. [[CrossRef](#)]
58. Bons, P.D.; Jessell, M.W. Micro-shear zones in experimentally deformed octachloropropane. *J. Struct. Geol.* **1999**, *21*, 323–334. [[CrossRef](#)]

